Japanese Journal of Applied Physics
Vol. 45, No. 3B, 2006, pp. 1913–1916

Scanning Tunneling Microscopy Combined with Hard X-ray Microbeam of High Brilliance from Synchrotron Radiation Source

Akira SAITO[1,2,3], Junpei MARUYAMA[1], Ken MANABE[1], Katsuyuki KITAMOTO[2,4], Koji TAKAHASHI[1], Kazuhiro TAKAMI[1], Shinji HIROTSUNE[5], Yasumasa TAKAGI[2], Yoshihito TANAKA[2], Daigo MIWA[2], Makina YABASHI[6], Masahi ISHII[6], Megumi AKAI-KASAYA[1,3], Shik SHIN[2,7], Tetsuya ISHIKAWA[2], Yuji KUWAHARA[1,2,3] and Masakazu AONO[1,3,8]

[1]*Department of Material and Life Science, Graduate School of Engineering, Osaka University, 2-1 Yamada-oka, Suita, Osaka 565-0871, Japan*
[2]*RIKEN/SPring-8, 1-1-1 Kouto, Mikazuki-cho, Sayo-gun, Hyogo 679-5148, Japan*
[3]*Nanoscale Quantum Conductor Array Project, ICORP, JST, 4-1-8 Honcho, Kawaguchi, Saitama 332-0012, Japan*
[4]*Department of Mathematical Sciences, Graduate School of Engineering, Osaka Prefecture University, 1-1 Gakuen-cho, Sakai, Osaka 599-8531, Japan*
[5]*Department of Physical Science, Hiroshima University, 1-3-1 Kagamiyama, Higashi-Hiroshima, Hiroshima 739-8526, Japan*
[6]*JASRI/SPring-8, 1-1-1 Kouto, Mikazuki-cho, Sayo-gun, Hyogo 679-5198, Japan*
[7]*ISSP, University of Tokyo, Kashiwanoha, Kashiwa, Chiba 277-8581, Japan*
[8]*Nanomaterials Laboratory, National Institute for Materials Science, 3-13 Sakura, Tsukuba, Ibaraki 305-0003, Japan*

(Received July 4, 2005; accepted October 5, 2005; published online March 27, 2006)

In situ scanning tunneling microscopy (STM) with highly brilliant hard X-ray irradiation was enabled at SPring-8. To obtain a good signal-to-noise ratio for elemental analysis, an X-ray beam with a limited size of $\varphi 10\,\mu m$ was aligned to a specially designed STM stage in ultrahigh vacuum. Despite various types of noises and a large radiation load around the STM probe, STM images were successfully observed with atomic resolution. The use of a new system for elemental analysis was also attempted, which was based on the modulation of tunneling signals rather than emitted electrons. Among tunneling signals, tunneling current was found to be better than tip height as a signal to be recorded, because the former reduces markedly the error of measurement. On a Ge nanoisland on a clean Si(111) surface, the modulation of tunneling current was achieved by changing the incident photon energy across the Ge absorption edge. [DOI: 10.1143/JJAP.45.1913]

KEYWORDS: STM, X-ray, synchrotron radiation, elemental analysis, Ge, island, Si(111)

1. Introduction

Despite extensive development of scanning tunneling microscopy (STM) for more than 20 years, it is still difficult to identify chemical species by STM. Many methods have been proposed for elemental analysis using STM such as, tunneling spectroscopy,[1)] and the use of work function,[2)] STM image contrast,[3)] and image states.[4)]

Other approaches with STM including a local optical spectroscopy or related topics such as light illumination,[5)] and light emission[6)] have achieved some positive results for distinguishing between different chemical states, via optically excited vibrational or electronic states with the spatial resolution of STM.[7)]

Although these approaches are successful and valuable examples, they are limited in generality or spatial resolution. Other experiments on inelastic tunneling spectroscopy[8)] or capacitance analysis[9)] are appropriate for analyzing chemical states, but not for the direct elemental identification. These difficulties often make the interpretation of STM images ambiguous.

In order to obtain general elemental information difficult to obtain solely by STM, the combination of STM with the use of X-rays appears attractive. This is because X-rays can excite core electrons specific to elements and their chemical state, by tuning the energy of X-rays to a specific binding energy. From this viewpoint, a series of experiments has been attempted for X-ray excited STM, where a probe tip was used for collecting emitted electrons.[10,11)] Currently, this method leads to a relatively limited spatial resolution because it detects photoexcited electrons emitted from a wide area. Atomic force microscopy (AFM) was also attempted under synchrotron radiation (SR) irradiation, but the resolution was not clear.[12)]

In this paper, we show an approach that is different from the past SR-based STM (SR-STM) measurement techniques, which uses a system developed for *in situ* SR experiments. To obtain local information on the nanometer order, we focused on monitoring the modulation of tunneling signals, rather than emitted electrons. To extract such a weak signal, the key point is to increase signal-to-noise (S/N) ratio, which was realized by preventing excessive excitation and monitoring directly tip current under the tunneling conditions, instead of tip motion. S/N ratio and experimental error were greatly improved, and the modulation of the signal was achieved on Ge nanoisland on a Si(111) surface by changing the incident photon energy across the Ge absorption edge.

2. Experimental

To take advantage of X-ray excitation, we still have a serious difficulty, i.e., the minute probability of core excitation. This might be one of the reasons the number of STM studies related to X-ray excitation are quite limited. To prevent this difficulty, we used SR of the highest brilliance, $\sim 10^{12}$ more intense than that of the conventional X-ray tube. The apparatus was installed at the beamline BL19LXU[13)] of SPring-8 that provides the most brilliant hard X-rays of approximately 2×10^{14} photons/s under the monochromated condition with a beam dimensions of $V \times H = 500 \times 1000\,\mu m^2$ at the sample position. Here, brilliance, which can be expressed as photon density, is more essential than the total flux of the incident beam.

On the other hand, the high brilliance leads to some

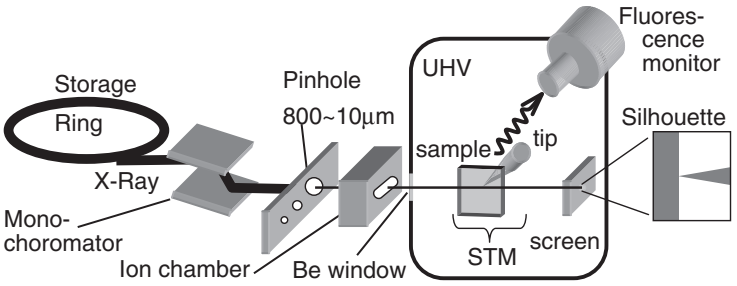

Fig. 1. Schematic view of experimental geometry.

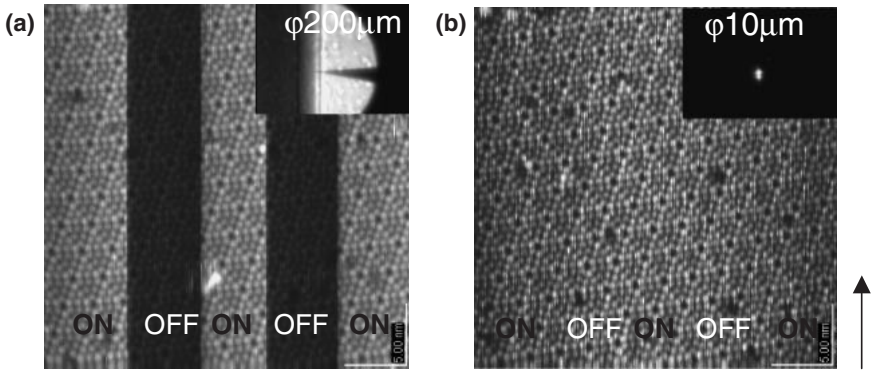

Fig. 2. STM images ($30 \times 30\,\mathrm{nm}^2$ for both) of clean Si(111) surface with on-off switching of X-ray irradiation with sample bias (V_s) = 1.5 V and tunneling current (I_t) = 0.3 nA. The X-ray beam size is φ 200 μm (left) and φ 10 μm (right), as shown in the inset with silhouette images. The arrow represents the scanning direction.

disadvantages: thermal and electrical noises, damage around the STM scanner or sample, and instability of the system such as thermal drift. The point of the experiments is how to adjust the incident beam to be as small as possible at the STM observation point in order to avoid excessive irradiation and obtain a high S/N ratio.[14] For this purpose, the total reflection condition with a grazing incident angle of X-rays from the sample surface is important, because it can limit the penetration depth of X-rays into the substrate to ~3 nm. The ideal ambient experimental condition is ultra-high vacuum (UHV) rather than gases or air to prevent the unnecessary excitation of many electrons that produces noise. In addition, the alignment must be performed as fast as possible due to the limited machine time at the SR facility.

We developed an STM system that enables an *in situ* experiment on highly brilliant X-ray beams of φ 10 μm aligned at the STM observation point in UHV with an accuracy of 1 μm. For this purpose, the system is composed of a multi axis stage for an accurate three-body (microbeam, tip end, and sample surface) alignment and also a monitoring system for the alignment using a silhouette of the sample and tip in the X-ray beam (Fig. 1). Details of the system are described elsewhere.[15] The STM controller and scanner were based on a conventional STM system (JEOL, Tokyo, Japan). The sample stage was set in an UHV chamber with a base pressure of 1.5×10^{-8} Pa. The STM tip was made from tungsten wire (φ 0.3 mm) by electrochemical etching in NaOH solution.

Despite a noisy condition in the experimental hutch of the SR facility and a large radiation load around the probe tip, STM images were successfully obtained with atomic resolution (Fig. 2). Figures 2(a) and 2(b) show STM images of a Si(111) 7×7 clean surface (n type, 4–7 Ω cm) in the constant-current mode with the on-off switching of the X-rays, where the insets show the silhouettes in the beam of φ 200 μm (a) and φ 10 μm (b). The energy of the incident beam was 16.5 KeV at an incident angle of 1.5° from the sample surface.

The bright bands in Fig. 2(a) correspond to the beam-irradiated states. Since the images were obtained in the constant-current mode, the bright band indicates that the tip is retracted due to X-ray irradiation. The origin of this stripe can be ascribed to electron emission, surface photovoltage, or the thermal effect. This modification of the image markedly disrupts the signal in our case. However, the modification of the image was effectively removed using an aperture of φ 10 μm without decreasing the incident photon density [Fig. 2(b)].

Even with the limited beam size of φ 10 μm, the concomitant emission produced by X-ray irradiation decreases spatial resolution markedly. A countermeasure is to develop a special tip probe that has a coaxial structure, of which only the center core of nanometer order is conductive to collect the emission from a limited area of nanometer size on the surface. However, from viewpoint of experimental efficiency, another method would be desirable. An appropriate signal other than emitted electrons must be a parameter localized at atomic resolution, i.e., tunneling gap or current. To distinguish a specific element, such tunneling signals must be compared between the different incident photon energies across the absorption edge of the

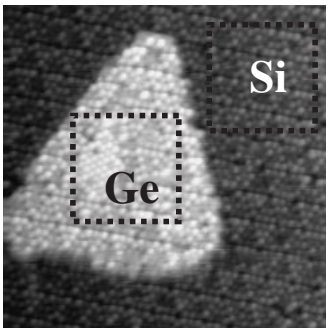

Fig. 3. Ge nanoisland measured to obtain energy dependence of topographic height [Fig. 4(b)] of Ge nanoisland with respect to surrounding Si substrate ($50 \times 50\,\mathrm{nm}^2$, $V_s = -2\,\mathrm{V}$, $I_t = 0.3\,\mathrm{nA}$).

element, in the same area on the sample. Here, the sample was a Ge nanoisland (Fig. 3), which was formed after annealing at 500 °C of 0.3 ML of Ge deposition on a clean Si(111) 7×7 surface.[16)]

First, we measured the energy dependence of the topographic height of the Ge nanoisland with respect to the surrounding Si area across the Ge absorption edge. The STM image of the area shown in Fig. 3 (constant-current mode, $I_t = 0.3\,\mathrm{nA}$) was taken repeatedly at each incident X-ray energy scanned in 1 eV steps from 11.106 to 11.115 KeV. For obtaining statistical accuracy, the average height of the same square dotted area shown in Fig. 3 was recorded both for the Ge nanoisland and surrounding Si area, and the height of the Ge nanoisland was obtained by subtracting that of the Si area at each step of the energy scan.

Second, we measured the energy dependence of tip current under the tunneling and X-ray irradiation conditions. The energy spectrum was obtained at a fixed point on the Ge island by scanning the incident X-ray energy.

3. Results and Discussion

Figure 4(a) shows a fluorescence spectrum obtained using a fluorescence monitor on the UHV chamber, and is a reference of X-ray energy and known as a fluorescence X-ray absorption fine structure (XAFS) profile. This profile, which is reproducible, guarantees energy stability and an accuracy higher than 1 eV at the beamline.

Figure 4(b) shows the energy dependence of the topographic height of the Ge island, which was recorded with respect to the height of the surrounding Si area. For comparison with the next current measurement, the relative change in tip height was converted to the change in tunneling current. Current–height conversion was achieved using an exponential current–height (I–Z) relationship, which was obtained by fitting the experimental I–Z data at $V_s = -2\,\mathrm{V}$ with an exponential function. Although the electrical and thermal noises have been removed as shown in Fig. 2(b), no step or peak was found around the energy of the Ge absorption edge.

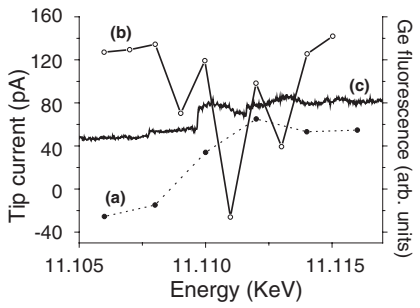

Fig. 4. Energy spectra of fluorescence yield (a: filled circles with dotted line), topographic height (b: open circles with solid zigzag line) of Ge island shown in Fig. 3, and tip current (c: solid profile) obtained on Ge nanoisland under tunneling conditions ($V_s = -2\,\mathrm{V}$, $I_t = 0.3\,\mathrm{nA}$). The profiles (b) and (c) are in a common vertical scale.

This is because the topographic data, which are based on the tip motion over several STM images, involve large errors due to the instable standard tip height that is markedly affected by the inclination and drift of the image for long periods of the experiment during the energy scan. Although tip height has been generally used in past studies of SR-STM,[10,11)] another strategy is to measure tip current under tunneling conditions. When the beam-induced change in tunneling current is recorded with respect to the tunneling current under beam-off condition, the accuracy will be improved by the stable standard base level of the signal. Also from the viewpoint of the faster response than the tip motion, tunneling current detection is desirable because the essence of the measurement is how to extract a small and fast change of the signal across the absorption edge.

A schematic diagram of the experimental system is shown in Fig. 5. An incident beam of φ 10 μm was chopped at a frequency of 3.0 kHz, and tip current was recorded through a lock-in amplifier (SEIKO, Tokyo, Japan) with integration for 20 ms to obtain a signal with a high S/N ratio. The high frequency also serves to effectively suppress the thermal expansion effect.

The incident beam was focused two-dimensionally to $V \times H = 200 \times 50\,\mu\mathrm{m}^2$ by a couple of mirrors to increase inner-shell excitation rate. The total reflection condition was an incident angle of 0.15° from the sample surface. Incident energy was scanned in 1 eV steps and all profiles were normalized by incident photon count. During the energy scan, we recorded tip motion and the magnified silhouettes of the tip and sample within the X-ray beam to check alignment conditions.

Figure 4(c) shows an energy spectrum of tunneling current under X-ray irradiation around the energy of the Ge absorption edge, in the same scale as that in Fig. 4(b) for comparison. The spectrum was obtained at a fixed point on a Ge nanoisland under a drift-free condition. Tunneling conditions were maintained in the constant-height mode to prevent a change in tunneling gap. The random dispersion in the spectrum was noticeably suppressed in comparison with that in Fig. 4(b). The improvement of the data indicates the high accuracy and small experimental error of the method.

As a result, a gap in tunneling current was observed across the Ge absorption edge, which was not confirmed in Fig. 4(b) due to the large error of the measurement. Tip current increases clearly above the Ge absorption edge, which reflects the excitation of the Ge atoms. The discrete jumps in current observed at 11.108 and 11.112 KeV are simply due to discrete changes in the monochromator condition that is scanned step by step during the continuous tip current measurement.

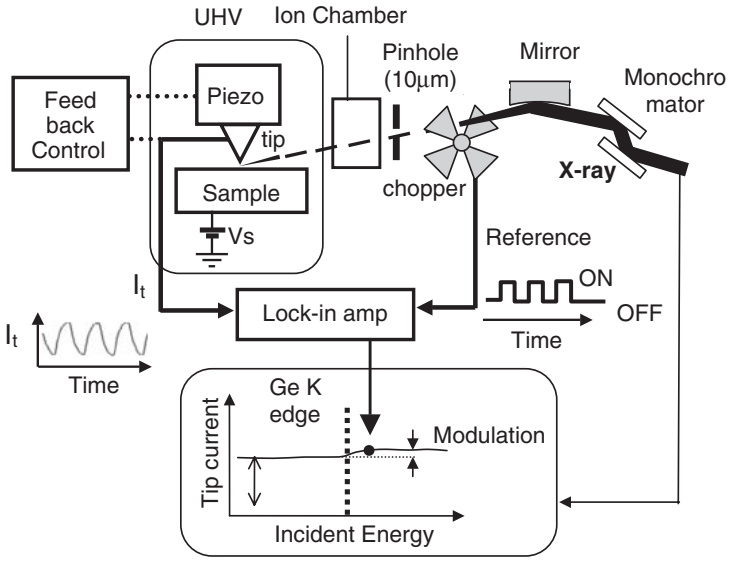

Fig. 5. Schematic diagram of tip current measurement system.

Although the signal might still contain many secondary electrons coming from the Ge atoms in a wide area, the clear current gap between 11.115 and 11.106 KeV gives us a premise to start elemental analysis, because such analysis is performed by comparing current gap among different surface sites. Actually, different current gaps were observed between the Ge nanoisland and the surrounding Si substrate.[15)]

This result indicates the possibility that tip current under tunneling conditions can differentiate the Ge nanoisland from the surrounding area, with the spatial resolution of STM. It is noted that STM is not only an analytical tool, but also serves for atomic manipulation. It has advantages over other techniques for spatial mapping by projecting emitted electrons using a lens system.[17)]

4. Conclusions

We attempted the elemental analysis by STM using a sample of Ge nanoislands on Si(111), which was based on the core-level interaction between the highly brilliant X-rays and surface atoms. To obtain local information, we focused on extracting the modulation of signals under tunneling conditions. To extract weak signals buried in various noises such as thermal and electrical noises and noise caused by emitted electrons, the key was to increase S/N ratio as much as possible. From this viewpoint, tunneling current was found to be more appropriate as a signal to be recorded than tip height, because the former reduces markedly the error of measurement. On a Ge nanoisland on a clean Si(111) surface, the modulation of tunneling signals was achieved by changing the incident photon energy across the Ge absorption edge.

Acknowledgment

We thank Dr. K. Kobayashi and Professors Y. Taguchi (Osaka Prefecture Univ.) and T. Sekitani (Hiroshima Univ.) for discussions, and Drs. K. Tamasaku, Y. Nishino, Y. Yoda (SPring-8), SPring-8 staff, and Y. Ogawa (Osaka Univ.) for experimental support. We thank Drs. H. Takada, K. Suzuki, S. Kitamura (JEOL Co., Ltd.), for technical support. This study was supported in part by a Grant-in-Aid for Scientific Research (No. 14702021) from the Ministry of Education, Culture, Sports, Science and Technology.

1) N. Papanikolaou, B. Nonas, S. Heinze, R. Zeller and P. H. Dederichs: Phys. Rev. B **62** (2000) 11118.
2) Y. Hasegawa, J. F. Jia, K. Inoue, A. Sakai and T. Sakurai: Surf. Sci. **386** (1997) 328.
3) M. Schmid, H. Stadler and P. Varga: Phys. Rev. Lett. **70** (1993) 1441.
4) J. Viernow, D. Y. Petrovykh, A. Kirakosian, J.-L. Lin, F. K. Men, M. Henzler and F. J. Himpsel: Phys. Rev. B **59** (1999) 10356.
5) K. Takada, M. Takeuchi and T. Takahashi: Jpn. J. Appl. Phys. **41** (2002) 4990.
6) A. Downes and M. E. Welland: Phys. Rev. Lett. **81** (1998) 1857.
7) S. Grafström: J. Appl. Phys. **91** (2002) 1717.
8) B. C. Stipe, M. A. Rezaei and W. Ho: Science **280** (1998) 1732.
9) M. Ishii: Phys. Rev. B **65** (2002) 85310.
10) K. Tsuji, K. Wagatsuma, K. Sugiyama, K. Hiraga and Y. Waseda: Surf. Interface Anal. **27** (1999) 132; Y. Hasegawa, K. Tsuji, K. Nakayama, K. Wagatsuma and T. Sakurai: J. Vac. Sci. Technol. B **18** (2000) 2676.
11) T. Matsushima, T. Okuda, T. Eguchi, M. Ono, A. Harasawa, T. Wakita, A. Kataoka, M. Hamada, A. Kamoshida, Y. Hasegawa and T. Kinoshita: Rev. Sci. Instrum. **75** (2004) 2149.
12) S. Suzuki, Y. Koike, K. Fujikawa, W. J. Chun, M. Nomura and K. Asakura: Chem. Lett. **33** (2004) 636.
13) M. Yabashi, T. Mochizuki, H. Yamazaki, S. Goto, H. Ohashi, K. Takeshita, T. Ohata, T. Matsushita, K. Tamasaku, Y. Tanaka and T. Ishikawa: Nucl. Instrum. Methods Phys. Res., Sect. A **467–468** (2001) 678.
14) A. Saito, Y. Kuwahara and M. Aono: 4th Int. Workshop on the Use of Coherent Soft X-rays from a 27 m Long Undulator at SPring-8, Hyogo, Japan, 2000, p. 129.
15) A. Saito, J. Maruyama, K. Manabe, K. Takahashi, K. Takami, M. Akai-Kasaya, Y. Kuwahara, K. Kitamoto, M. Yabashi, Y. Tanaka, D. Miwa, M. Ishii, S. Shin, T. Ishikawa and M. Aono: J. Synchrotron Radiat. **13** (2006) 216.
16) K. Masuda and Y. Shigeta: Appl. Surf. Sci. **175–176** (2001) 77.
17) Th. Schmidt, S. Heun, J. Slezak, J. Diaz, K. C. Prince, G. Lilienkamp and E. Bauer: Surf. Rev. Lett. **5** (1998) 1287.